CEDTECH International Journal of Environmental Science & Biotechnology
Volume 2, Number 4, December 2021
http: / /www.cedtechjournals.org
ISSN: 2756-4541

DISTRIBUTION OF URBAN HEAT ISLAND IN LAFIA LOCAL GOVERNMENT AREA: A GEOSPATIO-TEMPORAL APPROACH

[1*]Abubakar Alhassan. [1]Abejide Lewis Olumuyiwa, [1]Dahiru Mohammed Kabiru&[1]Fatima Sidi Sani
[1]Department of Geography, Faculty of Social Sciences,
Federal University of Lafia, Nasarawa State
Email: bakkarsoddeeq@gmail.com; olumuyiwaabejide@gmail.com,
dahirumk@gmail.com, fatimasidisani@gmail.com

ABSTRACT
This study is aimed at using remote sensing (RS) and Geographic Information System (GIS) to assess the urban heat island (UHI) in Lafia Local Government Area. A time series of Landsat data, from 1999 to 2020were used to extract the land surface temperature (LST), normalized difference vegetation index (NDVI) and normalized difference built-up index (NDBI). The study also examined the relationship between LST and (NDVI &NDBI) indices using correlation analysis. The results showed a considerable decrease in the mean LST from 32.13°C in 1999 to 30.97°Cin 2020, with a notable increase of 0.36°C between 2006 and 2013. It also established a positive relationship between LST and NDBI, and an inverse relationship between LST and NDVI. This implied that urban expansion and vegetation decrease influences the development of surface UHI through increased LST. Based on the results, urban planners should come up with effective planning and management of the urban centers. Also, policy makers are to come up with plans to provide thermal comfort in urban areas by increasing efforts in resuscitating urban vegetation and tree cover (tree planting), as well as encouraging the use of green and cool roofing sheet.

Keywords: *Land Surface Temperature (LST), Vegetation cover, Urban Heat Island (UHI)*

INTRODUCTION
Urban heat island (UHI) is the occurrence of higher temperatures in metropolitan areas in comparison to temperatures of suburban and rural areas, which means the higher the urbanization level the more prominent the UHI process (Pickett *et al*., 2011; Santamouris, 2013).The effect of UHI is caused by the spatial distribution of land surface temperature (LST), which is controlled by the heat flux on the surface and exacerbated

by urbanization (Dousset and Gourmelon, 2003; Sun*et al*., 2010). Thus, obtaining LST is critical for the analysis of UHI (Liuand Zhang, 2011).
The world has recently witnessed an increased urban population due to perceived socio-economic opportunities in cities, contributing to rapid urbanization (Sarif, *et al*., 2020). The global population in urban centers and cities has grown from 1.731 billion inhabitants (39.35%) in1980 to 3.968 billion (53.91%) in 2015, and is further predicted to over 9.725 billion (68%) by2050 (UNDES, 2019). The projection indicates that 35% of this growth is expected to occur in Africa and Asia in the next three decades. The consequence of this growth is the tremendous changes in land use/land cover (LULC) pattern and the alteration of various biophysical climatic conditions, particularly the Surface UHI that is measured using land surface temperature (LST) (Ranagalage*et al*., 2018, Wang &Derdouri, 2018). The transformation of land-use such as wetlands, vegetation, and agricultural areas into built-up and impervious surfaces can considerably influence LST (Kafy*et al*., 2020). Therefore, land use/land cover change dynamics are crucial factors influencing surface UHI due to the unique qualities (i.e., surface reflectance and roughness)attributed to each LULC category regarding its radiation and absorption energy (Tao*et al*., 2020).

The advent of satellite remote sensing technology has made it possible to study UHI both remotely and on continental or global scale. The most common satellite-derived indexes for estimating spatio-temporal variations of land surface temperature (LST) are the Normalized Difference Vegetation Index (NDVI) and the Normalized Difference Built-up Index (NDBI)using various remote sensing data such as NOAA AVHRR with 1.1km spatial resolutions, Landsat Thematic Mapper (TM), Enhanced Thematic Mapper Plus (ETM+) and Operational Land Imager (OLI) thermal infrared (TIR) bands with 120m and 60m spatial resolutions (Kumar and Shekhar, 2015). Previous studies have analysed the different relationships between LULC, LST, NDVI, and NDBI. In Shenzhen city, located in China's Pearl River Delta, a negative correlation was established between NDVI and LST, while the connection between LST and NDBI was positive (Chen, *et al*., 2006). A study in Tehran's Metropolitan city indicated a negative correlation between vegetation index and land surface temperature (Bokaie&Zarkesh, 2016). Similar studies in Akure, Ondo State, Nigeria (Aremu, *et al*., 2017);Sivas city, Turkey (Karakus, 2019); Egypt's greater Cairo region (Aboelnour& Engel, 2018) and some megacities of southern Asia such as Bangkok

(Thailand), Manila (Philippines) and Jakarta (Indonesia) (Estoque*et al*., 2018) revealed significant interactions, more precisely negative correlation, between land surface temperature and NDVI and a positive correlation between LST and built-up surfaces.

Although several studies exist on the spatio-temporal analysis of LST changes and their influence on vegetation and built-ups of Nigeria's rapidly growing cities are still relatively limited to non-existent. Lafia, the Nasarawa State capital has been under tremendous expansion over the last decade, with pressure in acquisition of space due to the establishment of Federal University of Lafia in 2011.In comparison to other developing cities in the Nigeria, Lafia has rapidly experienced various LULC changes, mainly an increasing built-up area and decreasing vegetation. The continuous alteration of land-uses for residential, commercial, industrial, and educational activities often contributes to climate change, particularly global warming, through increased UHI. However, in order to understand how surface UHI could be reduced in Lafia and its environs, vis-à-vis the study of LULC changes over time and its relationship with LST, hence, the justification for the study. Therefore, the study aimed to analyse the spatio-temporal distribution of land surface temperature of Lafia LGA, using satellite datasets and GIS techniques. To achieve the set aim: 1) the distribution of LST, NDVI, and NDBI was mapped and analysed, 2) the correlation analyses of LST, NDVI and NDBI satellite-derived indices were carried out.

The Study Area

Lafia is located between latitudes 8˚20'N-8˚38'N and between longitudes 6˚34'E-7˚30'E. It shares boundaries with Nasarawa Eggon and Wamba Local Government Area (LGAs) in the North, Obi LGA in the South East, Doma LGA in the South-West, Kokona LGA in the West and Plateau state in the East respectively (Figure 1). Climatologically, Lafia is characterized by a sub-humid climate with two distinct seasons: wet season occurs between May to September while the dry season falls between October and April. Ecologically, it is also known to have the southern Guinea Savanna vegetation, with an annual precipitation range of 1000mm to 1500mm and mean annual temperature range of 24°C to 33°C. The vegetation of Lafia is characterized by scattered trees with abundant woody shrubs and grasses. The soil is mostly sandy loam while few areas are with clayey loam. The geomorphology of the area comprised of the basement complex formation, with undulating lowlands

and network of hills developed on granites, magnetite rocks, which are believed to be plutonic in nature but later exposed to the surface by geomorphic processes. The most widely cultivated crops include the maize, rice, cowpea, guinea corn, sesame and sugar cane. The use of wetlands for irrigation farming during the dry season is also very paramount in Lafia.

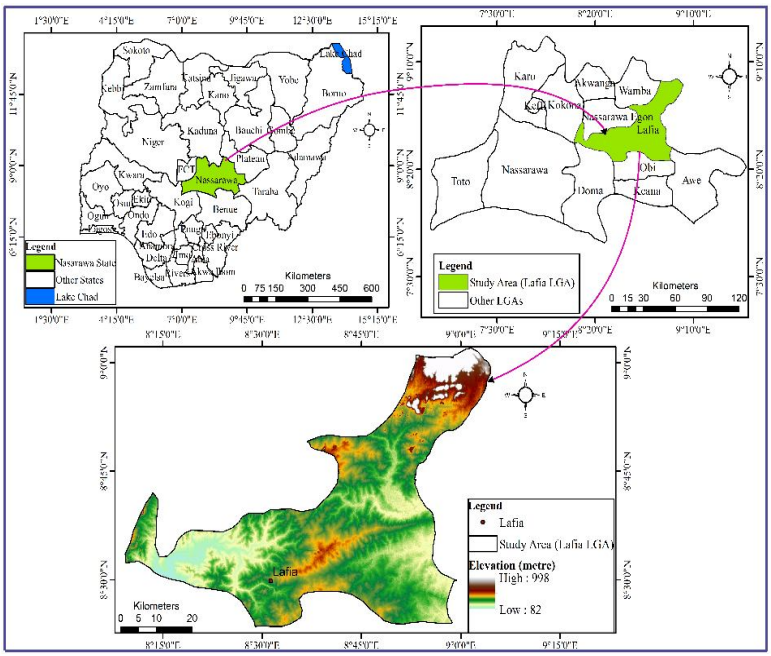

Figure 1: The Study Area: Lafia LGA, Nasarawa State
Source: GIS Laboratory, Dept. of Geography, FULafia (2021)

MATERIALS AND METHOD

Satellite Imagery Acquisition

In this study, a series of multi-temporal of Landsat datasets were downloaded from United States Geological Survey (USGS) Data Centre website (https://www.earthexplorer.usgs.gov) accessed on 15th June, 2021. The imagery comprise of Landsat-7 Enhanced Thematic Mapper (ETM+) of 1999, 2006 and Landsat-8 Operational Imager (OLI) & Thermal Infrared (TIR) of 2013 and 2020 are used in the analysis of urban heat island and vegetation changes over the study area. The whole study area belongs to path 188 and row 55. The characteristics of the images were summarized as shown in Table 1.

Table 1: Characteristics of the Landsat Datasets Used in the Study

Sensor	Sensor ID	Bands	Acquisition Date
Landsat-7 ETM+	LE07_L1TP_188054_19991113_20170216_01_T1	3,4, & 6	13th Nov.1999
	LE07_L1TP_188054_20061116_20170107_01_T1	3,4, & 6	16th Nov., 2006
Landsat-8 OLI/TIRS	LC08_L1TP_188054_20131111_20170428_01_T1	4,5, & 10	11th Nov., 2013
	LC08_L1TP_188054_20201114_20210314_01_T1	4,5, & 10	14th Nov., 2020

Estimation of Land Surface Temperature (LST)

The following steps and formulas are utilized for the processing of spatial distribution of LST from the thermal spectral bands of the Landsat imageries acquired.

3.2.1 Top of Atmospheric Spectral Radiance Calculation (TOA)

The first step of the algorithm is to input the thermal band and calculated spectral radiance formulated from the official site of USGS (Akher and Chattopadhyay, 2017) as shown in equation (1)

$$TOA(L) = M_L - Q_{cal} + A_l \qquad 1$$

Where TOA is the top of atmosphere spectral radiance, ML is the Band specific multiplication rescaling factor, Q_{cal} is the Radiant value corresponding to the thermal band and A_L is the Resizing factor

Conversion of Radiance to At-Sensor Temperature (BT)

After these reflection values are converted to radiance values, the spectral radiance is converted to brightness temperature (BT) using the thermal constants provided in the metadata file of the thermal band data (Akher and Chattopadhyay 2017) using equation (2)

$$BT = \frac{K_2}{(\ln(K_1/"TOA")+1)} - 273.15 \qquad (2)$$

Where BT is the brightness temperature, K_1 and K_2 are the band specific thermal conversion constants for Landsat-7 (Band 6) and Landsat-8 (Band 10) respectively.

3.2.3 Calculating the Proportion of Vegetation (Pv)

The vegetation rate can be calculated according to the following formula (Akher and Chattopadhyay 2017) using the equation (3).

$$P_v = ((NDVI - NDVI_{min})/(NDVI_{max} - NDVI_{min}))^2 \qquad (3)$$

Calculating Land Surface Emissivity (ε)

Land surface emissivity (ε) must be determined to calculate LST (equation 4). Surface emissivity is defined as the relative ability of the surface of a material to emit energy by radiation. The emissivity is also expressed as the ratio of the energy emitted by a given material to the energy emitted by a black body at the same temperature. In short, it is the efficiency of transmitting thermal energy from the surface to the atmosphere (Jimenez- Munoz *et al*. 2006).

$$\varepsilon = 0.0004 \times P_v + 0.986 \quad (4)$$

Where $\varepsilon$is the emissivity and P_v is the proportion of vegetation.

Calculation of Land Surface Temperature (LST)

Finally, Equation 5 and 6 are applied to obtain the land surface temperature map (Akher and Chattopadhyay, 2017).

$$LST = \frac{BT}{\{1+[(\lambda BT/\rho)*\ln(\varepsilon)]\}} \quad (5)$$

$$\rho = h\frac{c}{\sigma} = 1.438 \times 10^{-2} mK \quad (6)$$

Where σ is the Boltzmann constant (1.38×10^{-23}J/K), h is the Planck's constant (6.626×10^{-34}Js), and c is the velocity of light (2.998×10^{8}m/s).

Estimation of Normalized Difference Vegetation Index (NDVI)

The calculation of the normalized vegetation index was used both in the calculation of emissivity in the LST and the comparison of the existing vegetation areas between the LST (Equation 7) (Avdan and Jovanovska 2016).

$$NDVI = \frac{\rho_{NIR}-\rho_{RED}}{\rho_{NIR}+\rho_{RED}} \quad (7)$$

Where; ρ_{NIR} is the reflectance of near-infrared band and ρ_{RED} is the reflectance of red band

Estimation of Normalized Difference Built-Up Index (NDBI)

The normalized difference built-up index proposed by Zha*et al*. (2003) was used to identify the urban and built-up areas using equation 8.

$$NDBI = \frac{MIR-NIR}{MIR+NIR} \quad (8)$$

Where NDBI is the normalized difference built-up index (dimensionless), MIR is the mid-infrared band and NIR is the near-infrared band.

Determination of Correlations between LST on NDVI and NDBI

A total of 500 random points was generated and used to perform correlation analysis between LST, NDVI, and NDBI indices using Pearson's correlation coefficient in order to compare the influence of vegetation and built-up areas on urban heat island. This was calculated according to equation 9.

$$r = \frac{\sum_{i=1}^{n}(x_i-\bar{x})\times(y_i-\bar{y})}{\sqrt{\sum_{i=1}^{n}(x_i-\bar{x})^2}\sqrt{\sum_{i=1}^{n}(y_i-\bar{y})^2}} \quad (9)$$

Where r is Pearson's correlation coefficient, x_i measures values of the variable x, and y_i measures values of the variable y respectively. All the analyses were carried out using Arc GIS 10.5 and Microsoft Excel 2019 version Software.

RESULTS AND DISCUSSION

Land Surface Temperature Distribution

The spatio-temporal maps of the LST of Lafia LGA are presented in Figure 3 and quantified in Table 2 for the year 1999, 2006, 2013, and 2020. The results of the different periods revealed that the LST of the study area ranged between approximately24.36°C- 42.67°C, 22.84°C-42.23°C, 16.76°C-37.86°C, and 22.22°C-37.58°C during the four timeframes (i.e., 1999, 2006, 2013, and 2020, respectively).

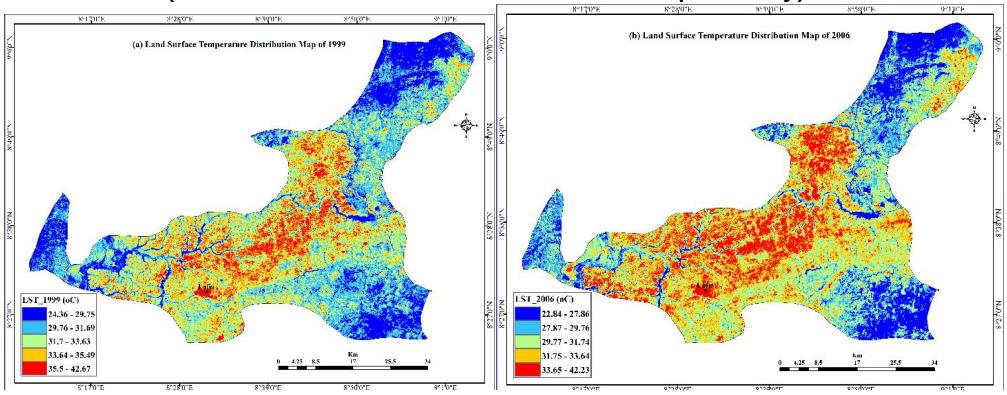

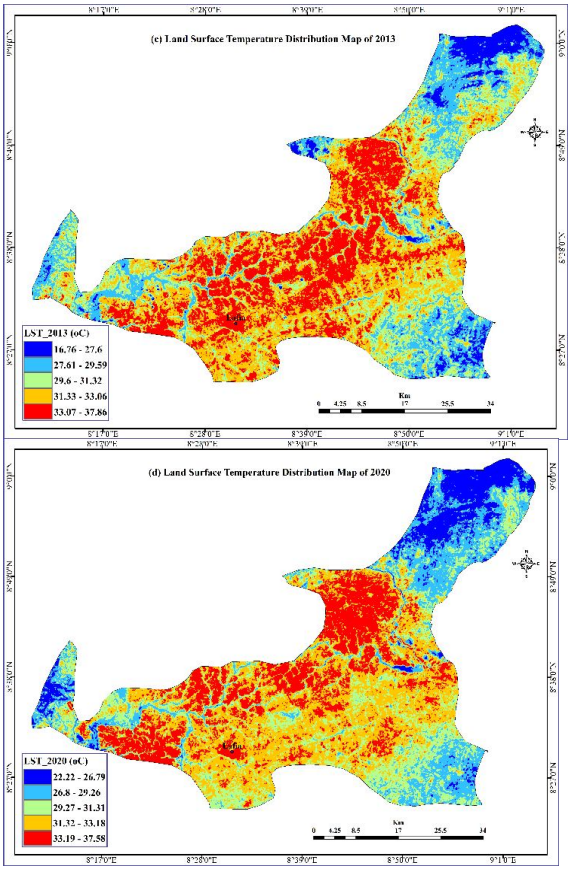

Figure 3: Spatio-temporal Distribution of LST (1999, 2006, 2013, &2020)
Source: Authors Computation (2021)

The LST analysis indicates that between 1999 and 2006, the mean LST has decreased by 1.14°C. A similar decrease of 0.38°C was observed between 2013 and 2020. However, the area witnessed an increase in the mean LST of 0.36°C between 2006 and 2013.

Table 2: Temporal Statistics of LST (°C) in Lafia (1999, 2006, 2013 and 2020)

S/No	Acquisition Date	Land Surface Temperature (LST)			
		Minimum (°C)	Maximum (°C)	Mean (°C)	Standard Deviation
1.	13th Nov.1999	24.36	42.67	32.13	2.51
2.	16th Nov., 2006	22.84	42.23	30.99	2.53
3.	11th Nov., 2013	16.76	37.86	31.35	2.17
4.	14th Nov., 2020	22.22	37.58	30.97	2.64

Source: Authors Computation (2021)

Normalized Difference Vegetation Index Distribution

The derived maps of the Normalized Difference Vegetation Index are presented in Figure 4 which portrays the four different study periods, i.e., 1999, 2006, 2013, and 2020. The statistical results are quantified and presented in Table 3. The characteristics of mean NDVI index over the study area was observed to decreased from 0.30 in 1999 to 0.20 in 2006, and 0.27in 2013 to 0.26 in 2020 respectively. The decrease in NDVI values is an indication of deforestation/ less vegetal cover or possibly as a result of an increase in agricultural activities. The implication of low vegetation cover will result in direct solar radiation and hence higher evaporation rate leading to inadequate moisture; these will have a detrimental effect on normal functions of the ecosystem. Therefore, there is need to enhance vegetation cover to curtail evapo-transpiration rate as well as increase moisture for the sustainability of wetland ecosystem. In the same way, the results also revealed that the highest NDVI values ranging between approximately 0.50 and 0.70, with such areas having mostly trees, shrubs, grasslands, and cultivated lands.

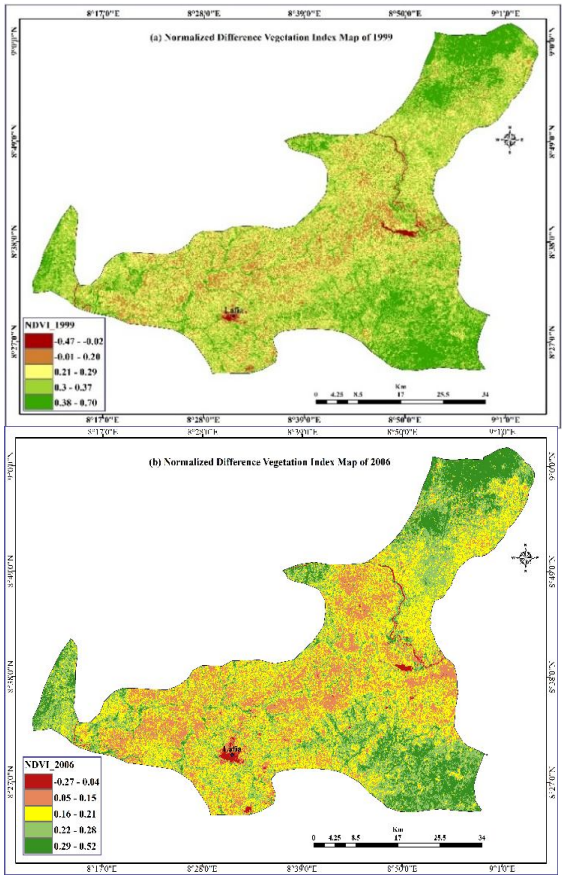

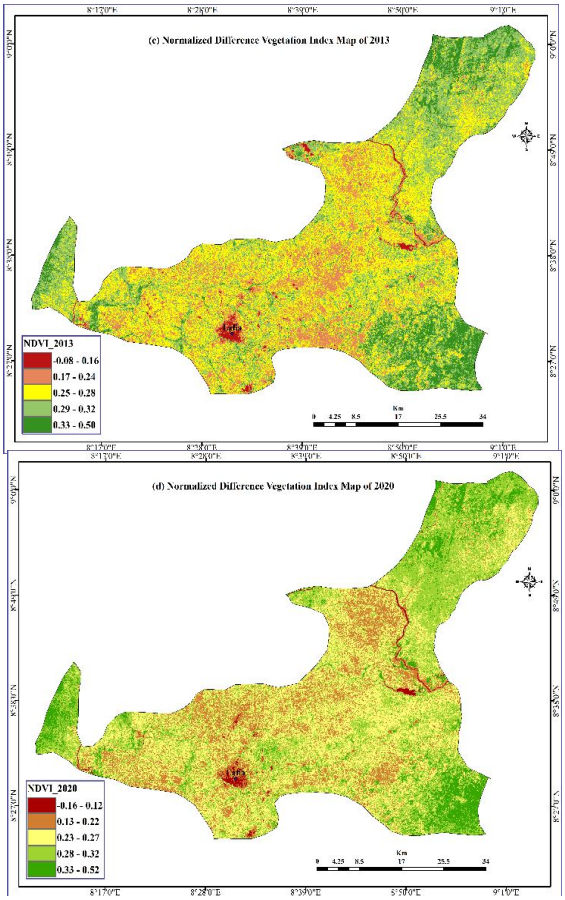

Figure 4: Spatio-temporal distribution of NDVI Maps (1999,2006, 2013, &2020)
Source: Authors Computation (2021)

Table 3: Statistics of NDVI in Lafia for the four periods between 1999 and 2020

S/No	Acquisition Date	Normalized Difference Vegetation Index (NDVI)			
		Minimum	Maximum	Mean	Standard Deviation
1.	13th Nov.1999	-0.47	0.70	0.30	0.09
2.	16th Nov., 2006	-0.27	0.52	0.20	0.07
3.	11th Nov., 2013	-0.08	0.50	0.27	0.04
4.	14th Nov., 2020	-0.16	0.52	0.26	0.05

Source: Authors Computation (2021)

Normalized Difference Built-Up Index Distribution

Figure 5 presents the NDBI maps of the study area for the year 1999, 2006, 2013, and 2020. The pixels with green pigments on the NDBI

maps were classified as having low values which represent places with low built-ups/pavement, pixels with yellow pigment were classified as having medium value which signifies areas with built-ups, while pixels with red colours on the NDBI maps with high values signifies area with built-ups of highest density. The zonal mean characteristics of NDBI values over the study area as presented in Table 4; revealed that the values are fluctuating from -0.20 to 0.14 in 1999 and 2006 and -0.05 to -0.02 in 2013 and 2020 respectively.

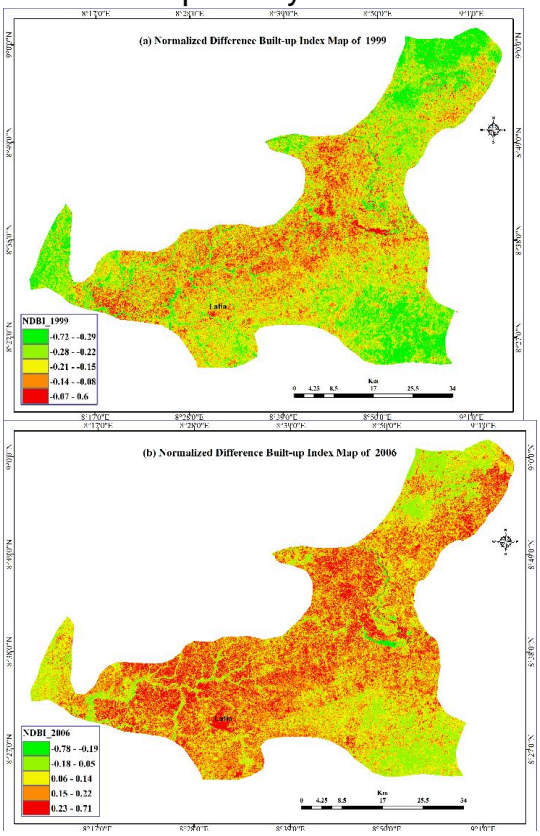

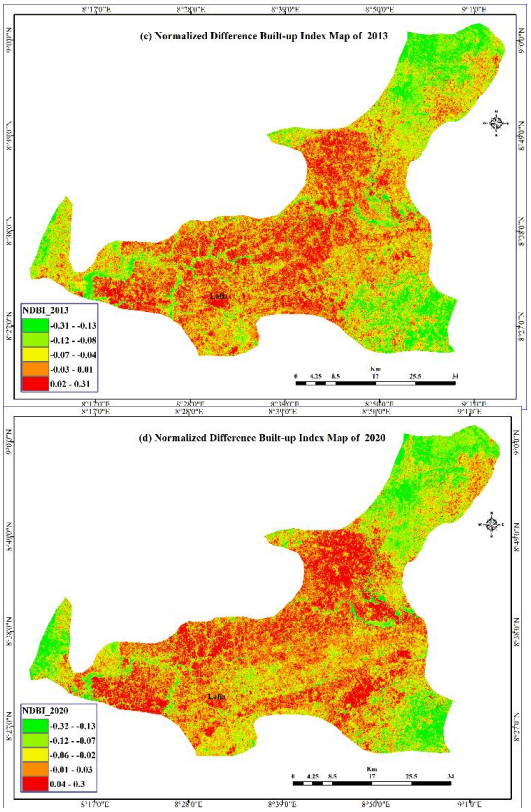

Figure 5: Spatio-temporal distribution of NDBI Maps (1999,2006, 2013, &2020)

Table 4: Statistics of NDBI in Lafia for the four periods between 1999 and 2020

S/No	Acquisition Date	Normalized Difference Built-up Index (NDBI)			
		Minimum	Maximum	Mean	Standard Deviation
1.	13th Nov.1999	-0.72	0.60	-0.20	0.08
2.	16th Nov., 2006	-0.78	0.71	0.14	0.10
3.	11th Nov., 2013	-0.31	0.31	-0.05	0.06
4.	14th Nov., 2020	-0.32	0.30	-0.02	0.07

Source: Authors Computation (2021)

Relationship between LST and NDVI Distribution

The correlation analysis between LST and NDVI was performed using Pearson's correlation coefficient, and the results are shown in Fig. 6 for the year 1999, 2006, 2013, and 2020. The results revealed a strong negative correlation, indicating that the NDVI has an inverse relationship with LST. This implies that areas with high NDVI values are related to lower temperatures, compared to areas with low values of NDVI. The scatter plots analysis results show a fluctuations in the determination coefficient during each period. This had a value (R^2) of approximately 0.39 in 1999, 0.49 in 2006, 0.28 in 2013, and 0.36 in 2020 respectively.

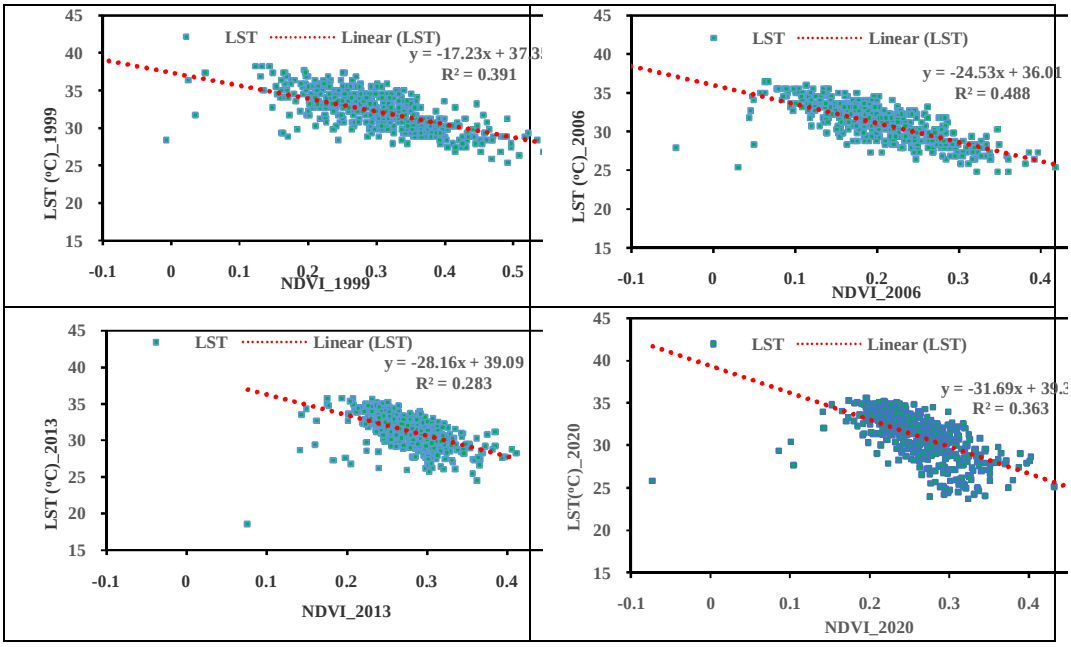

Figure 6: Relationship between LST and NDVI Distribution (1999, 2006, 2013, &2020).

Source: Authors Computation (2021)

Relationship between LST and NDBI Distribution

The graphical relationship between LST and NDBI is presented in Figure 7 for the year 1999, 2006, 2013, and 2020. It shows a positive association between LST and built-up areas. The scatter plots analysis results show a considerable increase in the determination coefficient during each period. This had a value (R^2) of approximately 0.28 in 1999, 0.40 in 2006, 0.64 in 2013, and 0.66 in 2020. However, results indicate that lower LST values corresponded to lower NDBI, while higher LST values corresponded to built-up areas of high density.

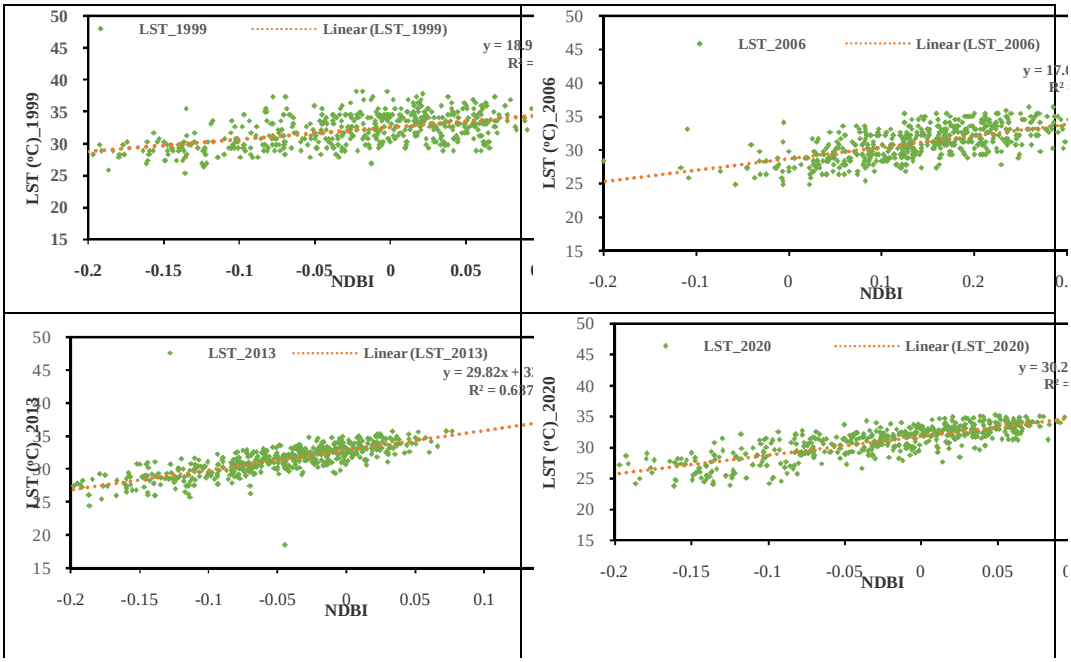

Figure 7: Relationship between LST and NDBI Distribution (1999,2006, 2013, &2020).
Source: Authors Computation (2021)

5. Conclusion

The study analysed the spatio-temporal distribution of UHI in Lafia LGA over the past 21 years (1999-2020) with the aid of remotely sensed data (Landsat satellite imageries). The change dynamics were mapped and quantified for four periods (1999, 2006, 2013, and 2020);in examining the spatial distribution of LST, NDVI, and NDBI. The correlation (R^2) values between LST versus NDVI and NDBI indices were computed. The LST analysis results revealed a considerable decrease in the mean

LST from 32.13°C in 1999 to 30.97°Cin 2020, with a notable increase of 0.36°C between 2006and 2013.The study also revealed a negative correlation between LST and NDVI while establishing a positive correlation between LST and NDBI during the different timeframes. In sum, it implies that higher LST is experienced along with a decline in vegetation and an increase in built-areas/impervious surfaces. Based on the above analyses, it is of paramount importance for the urban development agencies and planning authorities to adopt land-use strategies to mitigate the increasing surface UHI. In addition, policy makers should come up with plans to provide thermal comfort in urban areas by increasing the urban vegetation and tree cover, as well as encouraging the use of green and cool roofs.

REFERENCES

Aboelnour, M. & Engel, B. (2018). Application of Remote Sens. Techniques and Geographic Information Systems to Analyze Land Surface Temperature in Response to Land Use/Land Cover Change in Greater Cairo Region, Egypt. *J. Geogr. Inf. Syst.,* 10, 57–88.

Akher, S. K. &Chattopadhyay, S. (2017). Impact of urbanization on land surface temperature-A case study of Kolkata New Town. The International *Journal of Engineering Science,* 6(1), 71-81. DOI: 10.9790/1813-0601027181.

Aremu, O., Bello, E., Aremu, P., Aganbi, B., &Machoko, J. (2017). Monitoring and Analysis of Urban Heat Island using Remote Sensing Data – A Case Study of Akure, Ondo State, Nigeria. *Int J Environ Sci Nat Res.,*4(5): 555647. DOI: 10.19080/IJESNR.2017.04.555647.

Avdan, U. &Jovanovska, G. (2016). Algorithm for automated mapping of land surface temperature using LANDSAT 8 Satellite data. *Journal of Sensors.* Doi:10.1155/2016/148030

Bokaie, M., Zarkesh, M.K., Arasteh, P.D., &Hosseini, A. (2016). Assessment of Urban Heat Island based on the relationship between land surface temperature and Land Use/ Land Cover in Tehran. *Sustain. Cities Soc.,* 23, 94–104.

Dousset, B., &Gourmelon, F. (2003). Satellite multi-sensor data analysis of urban surface temperatures and landcover. *ISPRS J.*

Photogramm. Remote Sens. 58:43–54. http://dx.doi. org/10.1016/S0924-2716(03)00016-9.

Jimenez-Munoz, J.C., Sobrino, J.A., Gillespie, A., Sabol, D., & Gustafson, W.T. (2006). Improved land surface emissivities over agricultural areas using ASTER NDVI. *Remote Sensing of Environment,* 103(4), 474-487.

Kafy, A.A., Rahman, M.S., Faisal, A. A., Hasan, M.M., & Islam, M. (2020). Modelling future land use land cover changes and their impacts on land surface temperatures in Rajshahi, Bangladesh. *Remote Sens. Appl. Soc. Environ.,* 18, 100314.

Karakus, C.B. (2019). The Impact of Land Use/Land Cover (LULC) Changes on Land Surface Temperature in Sivas City Center and Its Surroundings and Assessment of Urban Heat Island. *Asia-Pac. J. Atmos. Sci.,* 55, 669–684.

Kumar, D. &Shekhar, S. (2015). Statistical analysis of land surface temperature–vegetation indexes relationship through thermal remote sensing. *Ecotoxicol. Environ. Saf.,* 121, 39–44.

Liu, L., & Zhang, Y. (2011). Urban Heat Island analysis using the Landsat TM data and ASTER data: a case study in Hong Kong. *Remote Sens.* 3:1535–1552. http://dx.doi.org/10. 3390/rs3071535

Murayama, R.C &Myint, Y.S.W. (2017) Effects of landscape composition and pattern on land surface temperature: An urban heat island study in the megacities of Southeast Asia. *Sci. Total Environ.,*577, 349–359.

Pickett, S.T.A., Cadenasso, M.L., Grove, J.M., Boone, C.G., Groffman, P.M., Irwin, E., Kaushal, S.S., Marshall, V., McGrath, B.P., Nilon, C.H., Pouyat, R.V., Szlavecz, K., Troy, A., & Warren, P. (2011). Urban ecological systems: scientific foundations and decade of progress. *J. Environ. Manag.* 92 (3):331–362. http://dx.doi.org/10.1016/j.jenvman.2010.08.022.

Ranagalage, M., Estoque, R., Handayani, H., Zhang, X., Morimoto, T., Tadono, T., & Murayama, Y. (2018). Relation between Urban Volume and Land Surface Temperature: A Comparative Study of Planned and Traditional Cities in Japan. *Sustainability*, 10, 2366.

Santamouris, M., (2013). Using cool pavements as a mitigation strategy to fight urban heat island: a review of the actual developments. Renew. Sust. Energ. Rev. 26:224–240. http://dx.doi.org/10.1016/j.rser.2013.05.047.

Sarif, M.O., Rimal, B., & Stork, N. (2020). Assessment of Changes in Land Use/Land Cover and Land Surface Temperatures and Their Impact on Surface Urban Heat Island Phenomena in the Kathmandu Valley (1988–2018). *Int. J. Geo-Inf.,* 9, 726.

Sun, Q., Tan, J., &Xu, Y. (2010). An ERDAS image processing method for retrieving LST and describing urban heat evolution: a case study in the Pearl River Delta Region in South China. *Environ. Earth Sci.* 59 (5), 1047–1055.

Tao, Y., de Leeuw, G., Zhao, L., Fan, C., Elnashar, A., Bashir, B., Wang, G., Li, L., Naeem, S., & Arshad, A. (2020). Modelling Spatio-temporal Land Transformation and Its Associated Impacts on land Surface Temperature (LST). *Remote Sens.*, 12, 2987.

United Nations Department of Economic and Social Affairs. World Population Prospects 2019 Volume I: Comprehensive Tables; United Nations Department of Economic and Social Affairs: New York, NY, USA, 2019.

Zha, Y., Gao, J., &NiI, S. (2003). Use of normalized difference built-up index in automatically mapping urban areas from TM imagery. *Int. J. Remote Sens.* 24 (3):583–594. http://dx.doi.org/10.1080/01431160304987.

Zhang, Y. (2006). Land surface temperature retrieval from CBERS-02 IRMSS thermal infrared data and its applications in quantitative analysis of urban heat island effect. *J. Remote Sens.* 10, 789–797.